Prototype tests for the ALICE TRD

A. Andronic, H. Appelshäuser, C. Blume, P. Braun-Munzinger, V. Cătănescu, M. Ciobanu, H. Daues, A. Devismes, Ch. Finck, N. Herrmann, T. Lister, T. Mahmoud, T. Peitzmann, M. Petrovici, A. Reischl, K. Reygers, R. Santo, R. Schulze, S. Sedykh, R.S. Simon, J. Stachel, H. Stelzer, J. Wessels, O. Winkelmann, B. Windelband, C. Xu
(for the ALICE Collaboration)

Abstract— **A Transition Radiation Detector (TRD) has been designed to improve the electron identification and trigger capability of the ALICE experiment at the Large Hadron Collider (LHC) at CERN. We present results from tests of a prototype of the TRD concerning pion rejection for different methods of analysis over a momentum range from 0.7 to 2 GeV/c. We investigate the performance of different radiator types, composed of foils, fibres and foams.**

Keywords— **Transition Radiation Detector, radiator performance, electron identification, pion rejection.**

I. Introduction

TRANSITION Radiation Detectors (TRDs) are being used in high energy experiments to improve the identification of electrons with respect to pions for momenta between ∼1 and 100 GeV/c (see [1] for a review on TRDs). A proposal to add a TRD [2] to the ALICE experiment [3] was approved in May 1999. By increasing the pion rejection power by at least a factor of 100 for momenta above 2 GeV/c, the TRD will allow, in conjunction with other ALICE detectors, to study, in the central region of the ALICE detector, various aspects of dielectron physics, among them the production of quarkonia like J/ψ, ψ' and the members of the Υ family, as well as the production of open charm and open beauty [2].

II. Detector characteristics

The ALICE TRD is composed of a radiator and a photon detector, the latter being a Drift Chamber (DC) with a 3 cm drift zone and an amplification region of 6 mm. To cope with the large charged particles multiplicities expected in Pb+Pb collisions at LHC and to provide the necessary position resolution for track reconstruction, the readout of the DC is done on a chevron pad plane [4]. We use the chevron width of 10 mm and the chevron step is tailored to the anode wire pitch of 5 mm. Each pad is connected to a preamplifier (PA) whose output is fed into a Flash-ADC (FADC), sampling with a frequency of about 20 MHz the drift time of up to 2 μs. The detection gas of the DC will be a Xe-based mixture to facilitate an efficient absorption of the transition radiation (TR) photons with typical energies between 4 and 30 keV. Six layers will surround the interaction point in full azimuth at radial distances from 2.9 to 3.7 meters and will match in polar angle the acceptance of the Time Projection Chamber ($45^\circ \leq \theta \leq 135^\circ$). A total number of 540 subdetectors will add up to a total surface of the TRD of about 800 m^2, with the largest single module of 1.22×1.56 m^2. With a pad size of 4.5-6 cm^2, the total number of channels will be up to 1.2 million, depending on the final geometrical configuration.

Manuscript received November 5, 2000.

A. Andronic, C. Blume, P. Braun-Munzinger, H. Daues, A. Devismes, Ch. Finck, R. Schulze, S. Sedykh, R.S. Simon and H. Stelzer are with Gesellschaft für Schwerionenforschung, D-64291 Darmstadt, Germany. (Correspondence to: Anton Andronic, GSI, Planckstr. 1, D-64291 Darmstadt, telephone: +40-6159-712769, e-mail: andronic@gsi.de).

H. Appelshäuser, N. Herrmann, T. Mahmoud, A. Reischl, J. Stachel, J. Wessels, B. Windelband and C. Xu are with Physikalisches Institut der Universität Heidelberg, D-69120 Heidelberg, Germany.

V. Cătănescu, M. Ciobanu and M. Petrovici are with NIPNE Bucharest, 76900 Bucharest-Magurele, Romania.

T. Lister, T. Peitzmann, K. Reygers, R. Santo and O. Winkelmann are with Institut für Kernphysik, Universität Münster, D-48149 Münster, Germany.

III. Results of prototype tests

A prototype of a DC with the characteristics presented above has been built at GSI. Apart from the mechanical realization, it differs from a final detector also concerning the surface, which is 0.5×0.6 m^2. We use W-Au anode wires of 20 μm diameter and Cu-Be cathode wires of 75 μm diameter. The entrance window of 25 μm aluminized kapton serves simultaneously as gas barrier and drift electrode.

A cross-section of a segment of one module of the TRD is shown in Fig. 1 along with a schematic illustration of the signals detected by the DC from a pion and an electron (with Lorentz factor γ >1000). The signal from TR photons produced in the radiator is superimposed to the signal from energy loss of electrons, as their angle with respect to the electron trajectory is very small (of the order of $1/\gamma$). The field lines in the DC, depicted in Fig. 1, are calculated with GARFIELD [6] for the dimensions mentioned above. The radiator is not to scale.

The prototype has been tested with Ar- and Xe-based gas mixtures, using a ^{55}Fe X-ray source of 5.9 keV, cosmic rays and mixed electron-pion beams provided by the secondary pion beam facility at GSI. Current- and charge-sensitive PAs were specially designed and built for these tests. For the results presented in the following the charge-sensitive PA was used. It has a gain of 2 mV/fC and a noise of about 2000 electrons rms. We use an 8-bit non-linear FADC system with 100 MHz sampling, integrated in the GSI-standard, VME-based data acquisition system,

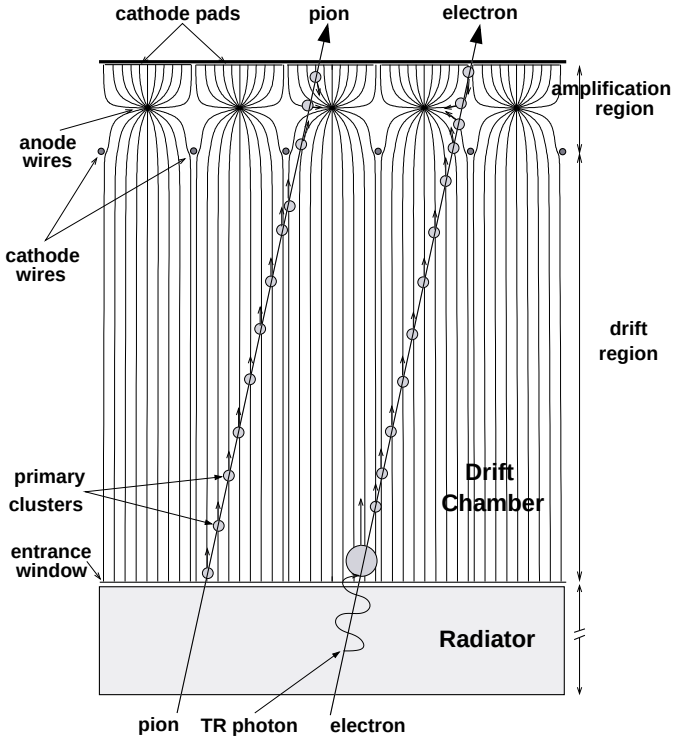

Fig. 1. The geometry of one TRD module. The geometric proportions and the field lines in the Drift Chamber (DC) are accurate. The radiator is not to scale. Schematic signals produced by a pion and an electron are shown.

MBS [5].

A. Source tests

The ^{55}Fe source was used to determine for the DC the optimum voltages and for measuring the gas gain and the energy resolution. By integrating the FADC pulse on three adjacent pads to account for the charge sharing, the energy resolution at the full energy peak of 5.9 keV is about 10%.

B. Beam tests

The setup used for the beam tests is sketched in Fig. 2. In addition to the DC and the radiator (R), the setup consisted of three scintillator counters (S0, S1, S2), a gas-filled threshold Cherenkov detector (Ch), two position-sensitive detectors (XY1, XY2) - either multiwire proportional chambers or silicon strip detectors - and a Pb-glass calorimeter (Pb).

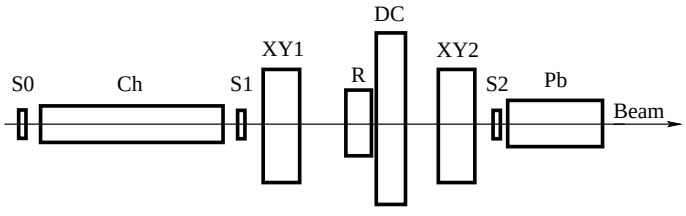

Fig. 2. The setup used for the beam tests (not to scale). The different components are explained in the text.

The measurements have been carried out at beam momenta between 0.7 and 2 GeV/c. The electron content of the beam varies as function of momentum, being of the order of 2-3% for 1 GeV/c. The beam trigger was defined by the S1 and S2 scintillator counters, to which the Cherenkov signal was added as the electron trigger. Both electron and pion events can be acquired during one spill by using appropriate pion scaledown factors. Off-line the events were selected using the correlation between the signals delivered by the Cherenkov and the Pb-glass detectors, shown in Fig. 3 for the momentum of 1 GeV/c. As seen, by requiring threshold energy deposits in both detectors (the lines in Fig. 3) one can isolate clean samples of pions and electrons. For this momentum we used a pion scaledown factor of 8.

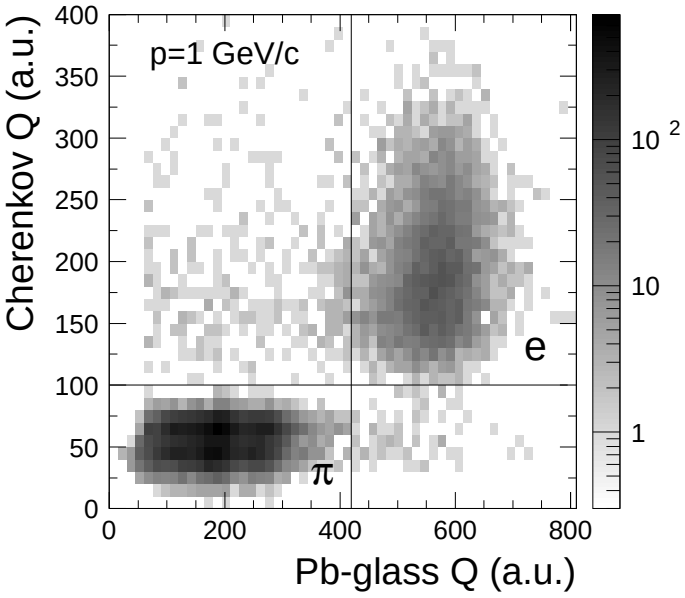

Fig. 3. The correlation of the signals from the Cherenkov detector and the Pb-glass calorimeter. The thresholds used to identify pions and electrons are plotted.

The gas mixture used for the DC was 90% Xe, 10% CH_4 and the voltages were U_d=-4.0 kV for the drift plane and U_a=1.6 kV for the anode wires. At these voltages the gas gain of the chamber was about 8000. The oxygen content in the gas was continuously monitored, being kept below 10 ppm using a flow of about 2 liters/hour.

TABLE I
THE PROPERTIES OF VARIOUS RADIATORS.

Name	Material	ρ (g/cm^3)	d (μm)
foils-1	PP	120 foils	20/500
foils-2	PP	220 foils	25/250
fibres-1	PP	0.09	17
fibres-2	PP	0.05	15-20
foam-1	PP	0.03	1300
foam-2	PP	0.06	700
foam-3	RC	0.11	$\leq$10
foam-4	RC	0.11	700
foam-5	PE	0.12	800

Different radiators were tested: regular foils of polypropylene (PP), mats of irregular PP fibres with various fiber diameters (between 15 and 33 μm) and foams of different material type: PP, polyethylene (PE) and Rohacell (RC). These radiators spanned a large range in densities and structural properties, as one can see in Table I, where we present their characteristics. The quantity d quoted here is the linear dimension of the structural unit, which for the foils means foil/gap thicknesses, for the fibres the diameter and for the foams the typical pore size. The thicknesses range is also large, from 3 to 10 cm. Unless otherwise specified, the *fibres-17μm* radiator employed for the following plots is the *fibres-1* radiator with X=0.3 g/cm^2.

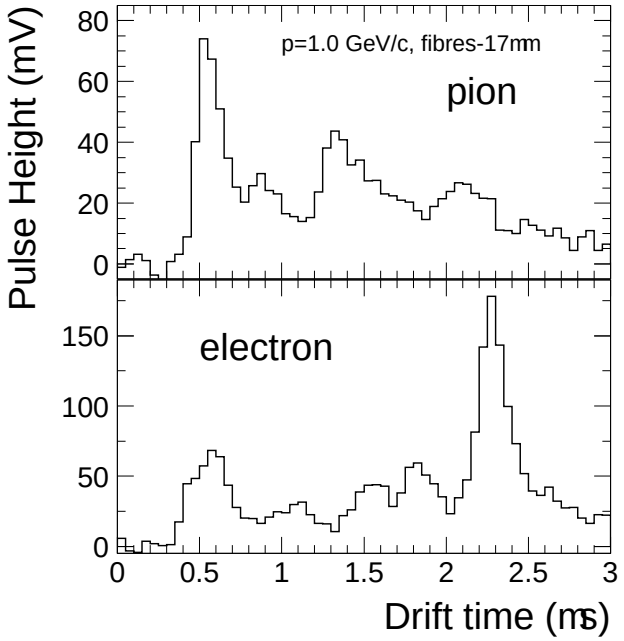

Fig. 4. Typical signals as function of drift time for pions and electrons for the momentum of 1.0 GeV/c. Note the different scales on the vertical axis.

Detailed simulations [2] showed that the electron identification is significantly improved by using, along with the pulse height, the drift time information. The need for FADCs is driven in addition by the necessary tracking capabilities in conjunction with the trigger option for electrons with momenta above 3 GeV/c [2]. In Fig. 4 we show an example of the signal distribution as a function of the drift time for a pion and an electron. Here and in all the subsequent analyses we are using a time bin of 50 ns, a value similar to the one in the final configuration of the TRD in ALICE. Note the different amplitude of the two signals and, for electrons, the big cluster at the late drift time, corresponding possibly to a TR photon absorbed early at the entrance of the DC (see Fig. 1). The time zero has been arbitrarily shifted by about 0.4 μs to have a measurement of the baseline.

We show in Fig. 5 the drift time distribution of the average pulse height summed over the adjacent pads, $\langle PH \rangle$, for pions and electrons in case of a fibre radiator with 17 μm fibre diameter (X=0.3 g/cm^2). For electrons (square symbols) there is a significant increase in the average pulse height at higher drift times, due to preferential absorption of TR at the entrance of the DC. Note that for pions (circles) the average pulse height in the drift region exhibits a slight increase as function of DC's depth. This is the result of build-up of detector currents from ion tails, convoluted in addition with the response of the preamplifier. The peak at the beginning of these distributions originates from the primary clusters in the amplification region, where the ionization is summed up in the same time channel from both sides of the anode wires (see Fig. 1). These features of the pion distribution have been reproduced by simulations using GARFIELD [6]. The dashed line in Fig. 5 is the expected pulse height distribution for electrons without TR; it has been obtained by scaling the pion distribution with a factor of 1.45, measured in a separate experiment without radiator.

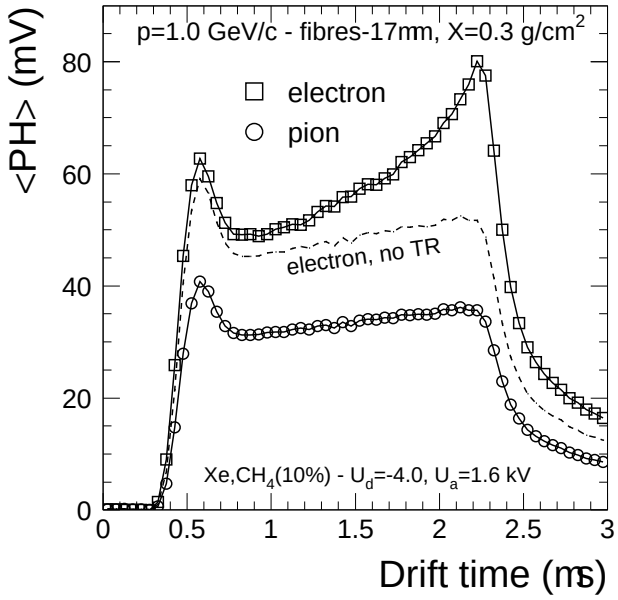

Fig. 5. Average pulse height as function of the drift time for pions and electrons for a radiator of 17 μm diameter fibres at the momentum of 1 GeV/c. The dashed line represents the energy deposit by pure ionization in case of electrons (see text).

Pulse height distributions as function of drift time were measured in other experiments [7], [8], [9], [10], however, the observed trends were somewhat different. A decrease of the pulse height as function of drift time was observed and it was attributed to electron attachment [10].

To study the relative performance of the various radiators presented in Table I we have classified them according to the equivalent thickness in two classes, with roughly X=0.3 g/cm^2 and X=0.6 g/cm^2 (for comparison, the radiation length for plexiglas is X$_0$=40.5 g/cm^2). The compilation of measurements for the two classes is presented in Fig. 6 in terms of the ratio between the average pulse height of electrons and pions, $\langle PH \rangle_e / \langle PH \rangle_\pi$, as function of detector depth. As the final number of required samples is yet to be specified by tracking performance considerations and due to statistics reasons as well, the detector depth is divided here in 4 drift zones, where each zone is

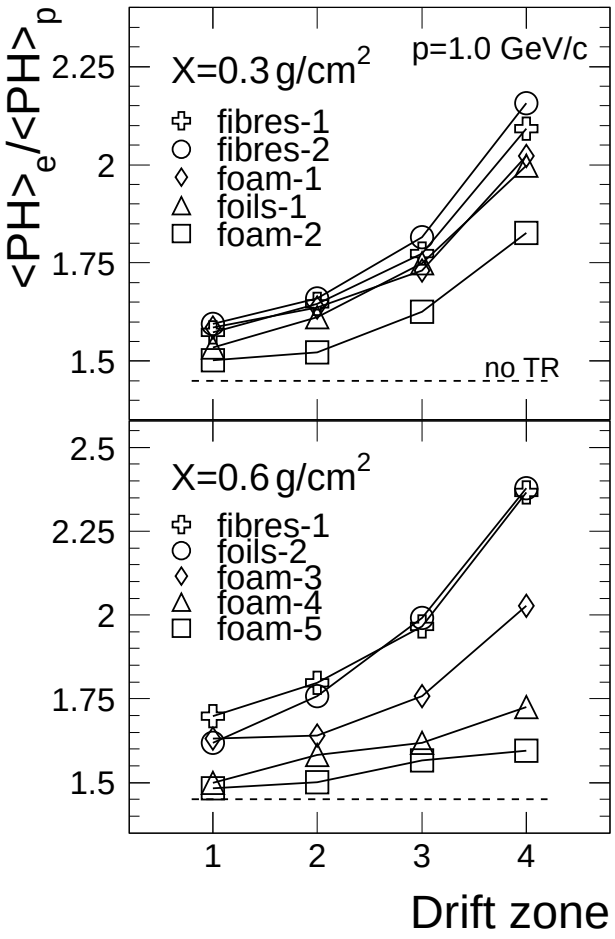

Fig. 6. Average relative electron/pion pulse height as function of the drift zone for various radiators of two thicknesses (see Table I) for the momentum of 1 GeV/c. Note the different scales on the vertical axis.

a quarter of the chamber's drift region (drift time between 0.75 and 2.35 μs in Fig. 5) and the numbering goes from the cathode wire plane towards the entrance of the DC. In this representation, a better relative performance of the radiator amounts to a higher ratio between electron and pion signal, while the increase towards the entrance of the detector gives information about the characteristics of the spectrum of the TR. The case of no TR would produce, for the present momentum value of 1 GeV/c, a flat distribution at about 1.45 (see above).

The most important conclusion from Fig. 6 is that the fibre radiators exhibit performances comparable to that of radiators with foils. Taking into account that the foil radiators (with X=0.22 g/cm^2 and X=0.5 g/cm^2, respectively) are significantly lighter than the other radiators in both cases, our conclusion is in agreement with previous studies [8]. The fibres with lower density, *fibres-2*, produce slightly more TR compared to the more dense ones, *fibres-1*. In a separate study we have found that the fibre diameter influences very little the TR yield. Radiators with fibres with 17 and 33 μm diameter show similar TR performance for the same density and thickness (see Fig. 7 below).

Concerning the foams, their performance is comparable to the fibres only in the case of the light PP foam, *foam-1*, however, with the disadvantage of a 10 cm thick radiator. The more packed version of the same material, *foam-2*, produces significantly less TR (furthermore, it is thicker, X=0.36 g/cm^2). The two Rohacell foams exhibit very different features. Contrary to the expectations, it is the version with less structure (invisible pores), *foam-3*, that gives higher TR yield. The other Rohacell foam, *foam-4*, as well as the PE foam, *foam-5*, are basically excluded as radiator candidates. Judging by their apparent structure, these foams would have been expected to deliver reasonably good TR performance. Their low TR yield may be the consequence of a higher absorption due to particular chemical compositions. It was found that even PE foil radiators exhibit poor TR performance [8]. In general, similar results concerning the relative comparison of different radiator materials have been obtained in other experiments [8], [11], [12].

A plexiglas 5.8 mm thick (X=0.66 g/cm^2) was used as dummy radiator and we have found that its contribution is essentially negligible. The results of the measurements for the dummy radiator and without radiator and the relative performance comparison of the 17 μm and 33 μm fibre radiators of identical thickness and density are summarized in Fig. 7.

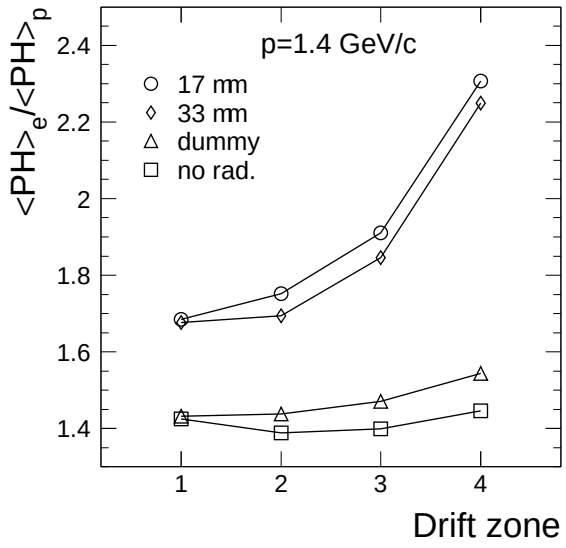

Fig. 7. Average relative electron/pion pulse height as function of the drift zone for 17 and 33 μm fibre radiators for the momentum of 1.4 GeV/c. Measurements without radiator and with a dummy one are shown for comparison.

The final choice of the radiator has to be a compromise between TR yield, total thickness of material and, given the large size and the difficult collider geometry of the ALICE TRD, mechanical considerations. We have already tested sandwich radiators composed of fibres and foams and have found that their performance can satisfy the above requests.

The distributions of the integrated energy deposit are shown in Fig. 8 for pions and electrons for the momentum of 1 GeV/c, in case of a 17 μm fibres radiator. The pure

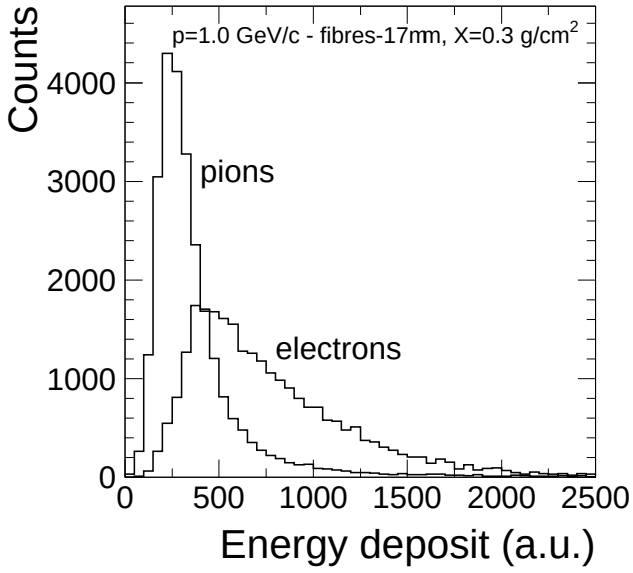

Fig. 8. Integrated energy deposit for pions and electrons for a momentum of 1.0 GeV/c. A radiator with 17 μm fibre has been used.

Landau distribution of pions is skewed towards higher values in the case of electrons by the contribution of the TR.

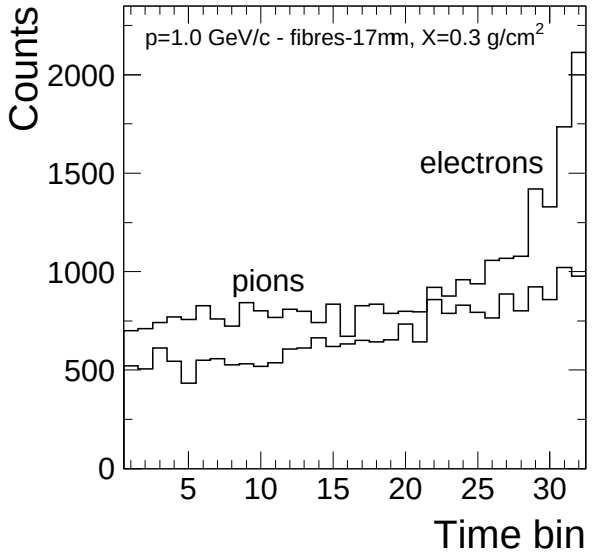

Fig. 9. The distributions of position of the largest cluster found in the drift region for pions and electrons. The momentum is 1.0 GeV/c and the radiator is 17 μm fibres.

The distributions of the position of the largest cluster found in the drift region are shown in Fig. 9. The detector depth is expressed here in time bin (of 50 ns) number, where the counting starts at 0.75 μs (see Fig. 5) and increases towards the entrance window for a total of 32 time bins. The trends seen in Fig. 5 are present in these distributions as well. For the case of electrons the probability to find the largest cluster is strongly increasing towards the entrance of the detector (higher time bin number) due mainly to the contribution of TR, while for pions there is only a slight increase which is due to the ion tail build-up explained above.

The distributions presented in Fig. 8 and Fig. 9 correspond to the same number of events. These distributions have been employed as probability distributions in simulations aimed at determining the pion rejection factor for the proposed configuration of the ALICE TRD. To extract the pion rejection factor we have studied three different methods: i) truncated mean of integrated energy deposit - TMQ; ii) likelihood on integrated energy deposit (see Fig. 8) - L-Q [13]; iii) bidimensional likelihood on energy deposit and position of the largest cluster found in the drift region of the DC (see Fig. 9) - L-QX [9]. We assume that the six layers have identical performance as represented by the measured distributions of Fig. 8 and Fig. 9. Both the truncated mean (the truncation is done by excluding the highest value of the integral energy deposit among the layers) and the likelihood (see i.e. [13], [14] for details) distributions were constructed over the six (independent) layers for the same number of simulated pion and electron events. Cuts of certain electron efficiency were involved at the end on these distributions and the pion efficiency is derived within these cuts. We note that another method, "cluster counting" [15] is widely used, in particular for "fine grain" TRDs like the ones used in ATLAS [16] and in HERA-B [17]. As was shown in [8], [9] and as our own simulations have demonstrated [2], the likelihood on integrated charge remains better than the cluster counting method.

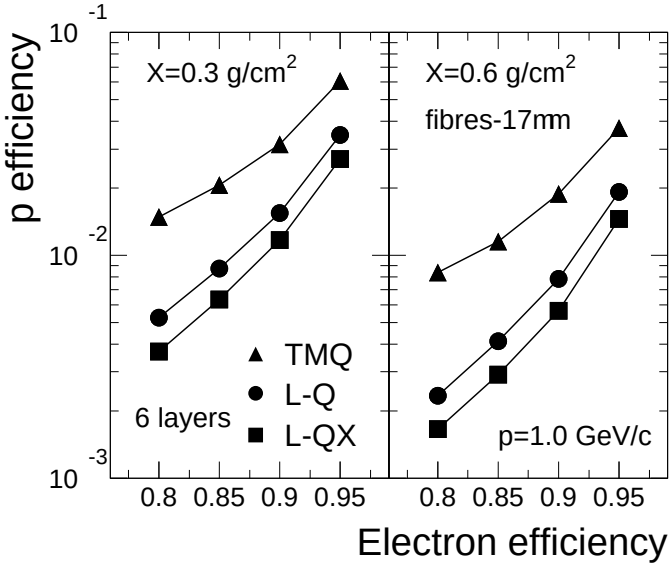

Fig. 10. The pion efficiency as function of electron efficiency determined with truncated mean on energy deposit (TMQ), likelihood on total energy deposit (L-Q) bidimensional likelihood on charge deposit and DC depth (L-QX).

In Fig. 10 we present the pion efficiency (the inverse of the rejection factor) as function of electron efficiency (90% electron efficiency is the commonly used value) in case of *fibres-1* radiators for the momentum of 1 GeV/c. The three methods introduced above are compared. The truncated mean method, although it delivers sizeably worse identification, has the advantage of being very easy to use, being advantageous especially for an on-line identification. The

bidimensional likelihood delivers the best rejection factor and will be studied further in order to optimize the final detector design. As emphasized earlier [9], the use of FADC to process the signals in a TRD can bring up to a factor of 2 in pion rejection power. In general, the three methods employed here give results in good agreement with earlier studies [8], [9].

By doubling the equivalent thickness of the radiator from X=0.3 g/cm^2 (left panel of Fig. 10) to X=0.6 g/cm^2 (right panel) one gains a factor of about 2 in pion rejection power. However, as discussed before, it remains to be seen how the additional material will influence (by producing secondary particles) the performance of the TRD itself and of other ALICE sub-detectors.

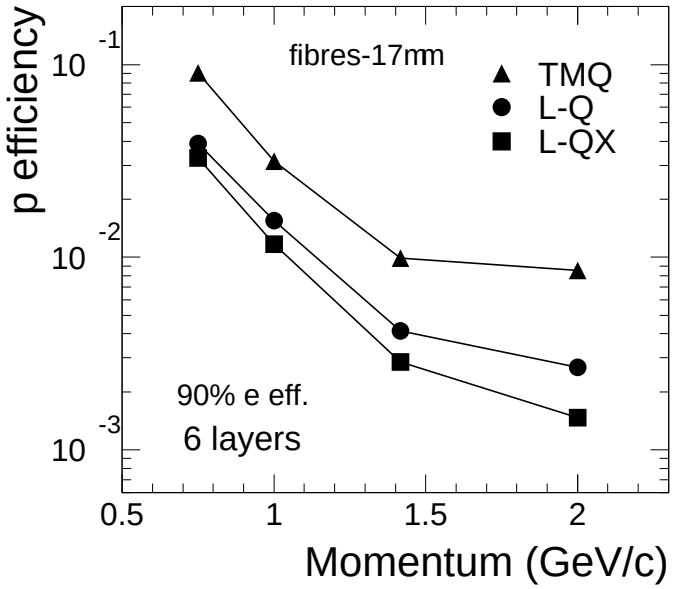

Fig. 11. Pion efficiency as function of momentum for a radiator with 17 μm fibres. The three methods used are discussed in the text.

The pion efficiency at 90% electron efficiency as function of momentum is shown in Fig. 11. The steep decrease of pion efficiency at momenta around 1 GeV/c is due to the onset of TR production [13], [14]. Towards our highest momentum value, 2 GeV/c, the pion efficiency reaches a saturation, determined by the TR yield saturation and by the pion relativistic rise. Due to these effects the pion rejection is expected to get slightly worse for momenta above 3 GeV/c [13], [7], [18], [8]. As one can see in Fig. 11, at momenta around 2 GeV/c the pion rejection factor of 300 to 500 achieved during these tests is above the required value for the ALICE TRD. However, one has to bear in mind that a significant worsening of TRD performance has been registered when going from prototype tests to real detectors [1]. This can be the effect of detector loads in a multiparticle environment. On the other hand, impressive pion rejection factors of 1000 and above have been achieved in full size TRDs in the NOMAD [14] and HERMES [19] experiments.

IV. Conclusions

We have presented results of test measurements with a prototype for the ALICE TRD. By studying different radiators we have been able to select the best candidates for the final radiator, which has to be the best compromise between TR performance and mechanical stiffness. Sandwich radiators composed of foam and fibres are currently under investigation.

The pion rejection capability was studied for different beam momenta and for different methods of data analysis. We have demonstrated that a rejection factor of about 500 (at an electron efficiency of 90%) for momenta around 2 GeV/c can be achieved using a fibre radiator of up to 5 cm thickness. Further work is underway, in particular devoted to the position resolution of the DC and to the performance of the detector in a high multiplicity environment.

Acknowledgment

We acknowledge the great help of N. Kurz on the data acquisition, of J. Stroth concerning the Si detectors and of M. Ardid for the assistance in data taking and data analysis.

References

[1] B. Dolgoshein, "Transition radiation detectors", *Nucl. Instr. Meth.*, vol. A326, pp. 434-469, 1993
[2] Addendum to ALICE Technical Proposal, CERN/LHCC 99-13, May 1999 (available at *http://www.gsi.de/∼alice*)
[3] ALICE Technical Proposal, CERN/LHCC 95-71, December 1995
[4] B. Yu, G. C. Smith, V. Radeka and E. Mathieson, "Investigation of chevron cathode pads for position encoding in very high rate, gas proportional chambers", *IEEE Trans. Nucl. Sci.*, vol. 38, no.2, pp. 454-460, April 1991
[5] H.G. Essel and N. Kurz, "The general purpose data acquisition system MBS", *IEEE Trans. Nucl. Sci.*, vol. 47, no.2, pp. 337-339, April 2000
[6] R. Veenhof, "GARFIELD, recent developments", *Nucl. Instr. Meth.*, vol. A419, pp. 726-730, 1998
[7] Y. Watase, Y. Suzuki, Y. Kurihara, H. A. Gordon, M. Diwan, R. E. Lanou and T. Shinkawa, "A test of transition radiation detectors for a colliding beam experiment", *Nucl. Instr. Meth.*, vol. A248, pp. 379-388, 1986
[8] R.D. Appuhn, K. Heinloth, E. Lange, R. Oedingen and A. Schlösser, "Transition radiation detectors for electron identification beyond 1 GeV/c", *Nucl. Instr. Meth.*, vol. A263, pp. 309-318, 1988
[9] M. Holder and H. Suhr, "Separation of electrons and pions by a transition radiation detector using Flash ADC", *Nucl. Instr. Meth.*, vol. A263, pp. 319-324, 1988
[10] J.-F. Detoeuf, Y. Ducros, F. Feinstein, J. R. Hubbard, P. Mangeot, B. Mansoulie et al., "The D0 transition radiation detector", *Nucl. Instr. Meth.*, vol. A265, pp. 157-166, 1988
[11] E. O'Brien, D. Lissauer, S. McCorkle, V. Polychronakos, H. Takai, C. Y. Chi et al., "A transition radiation detector which features accurate tracking and dE/dx particle identification", *IEEE Trans. Nucl. Sci.*, vol. 40, no.2, pp. 153-157, April 1993
[12] W. Brückner, T. Kallakowsky, H. M. Lauber, R. Michaels, S. Paul, B. Povh et al., "The transition radiation detector in the hyperon beam experiment WA89 at CERN", *Nucl. Instr. Meth.*, vol. A378, pp. 451-457, 1996
[13] A. Büngener, B. Koppitz, R. van Staa, P. Stähelin and M. Holder, "Electron identification beyond 1 GeV by means of transition radiation", *Nucl. Instr. Meth.*, vol. 214, pp. 261-268, 1983
[14] G. Bassompierre, S. Bunyatov, T. Fazio, J.-M. Gaillard, M. Gouanère, E. Manola-Poggioli et al., "Performance of the NOMAD Transition Radiation Detector", *Nucl. Instr. Meth.*, vol. A411, pp. 63-74, 1998

[15] C. W. Fabjan, W. Willis, I. Gavrilenko, S. Maiburov, A. Shmeleva, P. Vasiljev et al., "Practical prototype of a cluster-counting transition radiation detector", *Nucl. Instr. Meth.*, vol. 185, pp. 119-124, 1981
[16] T. Akesson, H. Carling, B. Dolgoshein, C. W. Fabjan, P. Farthouat, D. Froidevaux et al., "Particle identification performance of a straw Transition Radiation Tracker prototype", *Nucl. Instr. Meth.*, vol. A372, pp. 70-84, 1996
[17] V. Egorytchev, V. Saveliev, S.J. Aplin, "Particle identification via transition radiation and detectors", *Nucl. Instr. Meth.*, vol. A453, pp. 346-352, 2000
[18] H.-J. Butt, B. Koppitz, S. Nann and R. van Staa, "Electron identification up to 100 GeV by means of transition radiation", *Nucl. Instr. Meth.*, vol. A252, pp. 483-487, 1986
[19] K. Ackerstaff, A. Airapetian, N. Akopov, M. Amarian, V. Andreev, E. C. Aschenauer et al., "The HERMES Spectrometer", *Nucl. Instr. Meth.*, vol. A417, pp. 230-265, 1998